PLOS ONE

RESEARCH ARTICLE

Identification and characterization of soluble binding proteins associated with host foraging in the parasitoid wasp *Diachasmimorpha longicaudata*

Juan P. Wulff⊙*, Diego F. Segura, Francisco Devescovi, Irina Muntaabski, Fabian H. Milla, Alejandra C. Scannapieco, Jorge L. Cladera, Silvia B. Lanzavecchia⊙

Laboratorio de Insectos de Importancia Agronómica, Instituto de Genética Ewald A. Favret (INTA) gv IABIMO (CONICET), Buenos Aires, Argentina

* wulff.juan@inta.gob.ar

Abstract

The communication and reproduction of insects are driven by chemical sensing. During this process, chemical compounds are transported across the sensillum lymph to the sensory neurons assisted by different types of soluble binding proteins: odorant-binding proteins (OBPs); chemosensory proteins (CSPs); some members of ML-family proteins (MD-2 (myeloid differentiation factor-2)-related Lipid-recognition), also known as NPC2-like proteins. Potential transcripts involved in chemosensing were identified by an *in silico* analysis of whole-body female and male transcriptomes of the parasitic wasp *Diachasmimorpha longicaudata*. This analysis facilitated the characterization of fourteen OBPs (all belonging to the Classic type), seven CSPs (and two possible isoforms), and four NPC2-like proteins. A differential expression analysis by qPCR showed that eleven of these proteins (CSPs 2 and 8, OBPs 2, 3, 4, 5, 6, 9, 10, and 11, and NPC2b) were over-expressed in female antenna and two (CSP 1 and OBP 12) in the body without antennae. Foraging behavior trials (linked to RNA interference) suggest that OBPs 9, 10, and 11 are potentially involved in the female orientation to chemical cues associated with the host. OBP 12 seems to be related to physiological processes of female longevity regulation. In addition, transcriptional silencing of CSP 3 showed that this protein is potentially associated with the regulation of foraging behavior. This study supports the hypothesis that soluble binding proteins are potentially linked to fundamental physiological processes and behaviors in *D. longicaudata*. The results obtained here contribute useful information to increase the parasitoid performance as a biological control agent of fruit fly pest species.

Introduction

Chemical sensing plays a fundamental role in insect communication and reproduction, assisting behaviors such as host-seeking, feeding, mating, and avoidance of toxic substances [1]. Chemical compounds enter through pores in the sensilla cuticle and are then transported

through the lymph to sensory neurons assisted by water-soluble binding proteins [1]. Different
groups of such proteins have been described in insects: odorant-binding proteins (OBPs); che-
mosensory proteins (CSPs); protein members of the ML (MD-2 (myeloid differentiation fac-
tor-2)-related Lipid-recognition) family and odorant-degrading enzymes (ODEs) [1, 2]. These
binding proteins form a complex with odor molecules, which further interact with membrane-
bound receptors on the sensory neurons, such as odorant receptors (ORs), ionotropic recep-
tors (IRs), their corresponding co-receptors (ORco and IRco), gustatory receptors (GRs), and
sensory neuron membrane proteins (SNMPs) [1].

After the first OBP was discovered in *Antheraea polyphemus* Cramer (Lepidoptera: Satur-
niidae) [3], OBP homologous genes have been identified in many insect orders ranging from
12 to 100 identified proteins per species [4]. Members of this family can be grouped in more
than one category, such as Classic OBP, Minus-C type, and Plus-C type [5]. The Classic OBP
type (from which other variants can be defined) is a water-soluble protein of about 120–150
amino acids (10–30 kDa), expressed at a high concentration (10–20 mM) and with six highly
conserved cysteine residues in a characteristic position [6]. These cysteines form three disul-
fide bonds to stabilize a tertiary structure formed by six or seven α-helices that define a hydro-
phobic binding cavity, which may undergo changes in a pH-dependent manner [7]. CSPs are
very similar to OBPs in structure and function but characterized by four conserved cysteine
residues forming two disulfide bonds to stabilize five or six α-helices [8]. The first CSP was dis-
covered in *Drosophila melanogaster* Meigen (Diptera: Drosophilidae) showing high expression
in the olfactory sensilla of antennae [9]. This suggested a potential olfactory function, later
confirmed by semiochemical binding and electro-antennogram assays [10, 11]. The number of
genes for CSPs ranges from 4 to 70 per species [4], and there is no classification into
subfamilies.

The MLs are also water-soluble proteins, sharing several characteristics with CSPs and
OBPs [12]. These proteins (also known as NPC2-like proteins) possess a conserved domain
that can be found in about 100 protein families, such as myeloid differentiation factor 2 (MD-
2), Niemann-Pick disease protein type C2 (NPC2), and Ecdysteroid-regulated 16 kDa protein
(ESR16). NPC2-like proteins have been identified in different sensory structures in insects
[12–14], and their function as semiochemical carriers was confirmed in some species [15, 16].
NPC2s are the most widely studied ML proteins in insects and can be classified into three sub-
families, depending on the number of cysteine residues: six, seven, or eight [17]. The number
of NPC2 genes ranges from three to fourteen per species [4]. However, in some cases, the same
orthologous sequence has been classified into different subgroups (NPC2, ESR16 or MD-2), in
different Hymenoptera species [18, 19].

Recent studies have confirmed other important roles for soluble binding proteins in insect
biological processes. OBPs are also involved in metabolic functions, reproduction, or as a com-
ponent of the parasitic wasp venom [20–22]. CSPs are also associated with molting, mating,
and development [23, 24]. Some NPC2-like proteins are linked to molting as well as intracellu-
lar transport of sterols and spermatogenesis [25–27]. This supports the use of these genes as
potential targets to manipulate some fundamental behaviors at the species level [*e.g.* 28].

Parasitic wasps are important natural enemies of numerous species of insects, several of
which have achieved pest status in agricultural systems. Consequently, some parasitoid species
are important biological control agents used in integrated pest management programs [29].
Parasitic wasps find their hosts in the foraging environment by primarily using chemical cues
[30]. Recent studies on soluble binding proteins in parasitoids, such as *Microplitis mediator*
Haliday (Hymenoptera: Braconidae) and *Anastatus japonicus* Ashmead (Hymenoptera: Eupel-
midae), point to these genes/proteins as potential targets for manipulating fundamental behav-
iors [31, 32]. Although OBP studies are predominant, research on CSPs and NPC2-like

proteins has increased [12, 33]. This opens the possibility of exploring their genes /proteins to obtain efficient biological control agents, as an alternative to the use of chemical treatments against insect pest species [34].

Diachasmimorpha longicaudata Ashmead (Hymenoptera: Braconidae) is an endoparasitoid wasp considered the main biological control agent of Tephritidae fruit flies of economic importance. Females parasitize late instar larvae of several fruit fly species, such as *Ceratitis capitata* Wiedemann and *Anastrepha fraterculus* Wiedemann (Diptera: Tephritidae), which are important pests in several South American countries. Numerous ecological and behavioral studies have addressed key issues about the foraging behavior *of D. longicaudata* [35, 36], such as the identification of volatile organic compounds (VOCs) that are significantly attractive to females [37]. However, there are no studies on molecular mechanisms associated with this behavior. Therefore, information about the expression patterns of genes, possibly involved in the foraging behavior for oviposition in this parasitic wasp, constitutes the starting point to explore the underlying molecular mechanisms intervening in this process. This knowledge could contribute to increasing the field efficiency of *D. longicaudata* as a biological control agent of fruit fly species in the future.

The present study aimed at identification and first characterization of soluble binding proteins potentially associated with host foraging in *D. longicaudata*. The main hypotheses of this study were as follows: 1) during host foraging behavior, the female *of D. longicaudata* deploys soluble binding proteins to detect odors associated with the host; 2) the host detection and oviposition performance of *D. longicaudata* females can be modified by transcriptional silencing of some of these transcripts.

Materials and methods

Insect rearing

Parasitoids and fruit flies used in the study were obtained from the experimental rearing facility at Instituto de Genética "E. A. Favret" (IGEAF-INTA) gv-IABIMO (CONICET). Females of *D. longicaudata* used in the experiments were obtained from a colony reared on *A. fraterculus* for 25 generations. This colony was established from *D. longicaudata* insects reared on *C. capitata* for more than 200 generations and established with individuals from Fundación Miguel Lillo-CIRPON [38]. Insects were maintained under controlled rearing conditions [$25 \pm 2°C$, $65 \pm 5\%$ relative humidity (R.H.) and a 12:12 (light/dark) photoperiod] following protocols described by [35, 39]. Biosecurity considerations were in agreement with CONICET resolution 1619/2008 and with the WHO Biosecurity Handbook (ISBN 92 4354 6503). *A. fraterculus* larvae used for *D. longicaudata* rearing and behavioral assays were obtained from the experimental rearing facility at Instituto de Genética "E. A. Favret" (IGEAF, INTA) gv-IABIMO (CONICET).

Tissue collection, RNA extraction, and cDNA synthesis

Total RNA was extracted from three types of tissue of *D. longicaudata* adult individuals of both sexes: whole body (without antenna), antenna, and ovipositor (only females). Samples were stored in 600 µl of Trizol® reagent (Invitrogen Carlsbad, CA, USA) according to the manufacturer's specifications until RNA isolation. Specifically, we obtained five replicates of each pooled sample, as follows: "female body" included five whole bodies (without antennae) of 7- to 10-day-old naïve females; "male body" included five whole bodies (without antennae) of 7- to 10-day-old mated males;"male antenna" included the antennae of 30 males (7- to 10-day-old mated males), "female antenna" comprised the antennae of 30 females (7- to 10-day-old naïve females), and the "ovipositor" sample was composed of 30 ovipositors of 7-

to 10-day-old naïve females. In the case of females, naïve status represents mated adults with no experience in oviposition. This physiological condition was selected to analyze the basal expression of genes potentially associated with host foraging (to reduce the effect of other biological processes on olfaction, such as mating). The integrity of the extracted RNA was tested by using 1% w/v agarose gel electrophoresis visualized by ethidium bromide staining. In addition, the RNA samples were quantified by a ND-1000 spectrophotometer (Thermo Fisher Scientific-NanoDrop®, Wilmington, USA) at optical density (OD) 260 nm (2 μl of a 1:10 dilution).

From the aforementioned RNA samples, cDNA was synthesized by using the Improm-II Kit (Promega®, USA), according to the manufacturer's specifications and with temperature-cycling parameters, as follows: 70˚C, 5 min (1 cycle); 25˚C, 5 min (1 cycle); 37˚C, 120 min (1 cycle); 4˚C, 5 min (1 cycle).

Identification of putative soluble binding protein transcripts

A local tBLASTn [40] against a *D. longicaudata* whole-body transcriptome [41] was performed to identify candidate unigenes that encode soluble binding proteins associated with chemical communication. A database of soluble binding proteins (OBPs, CSPs, and NPC2s) was used as a query and recorded from the following species: *D. melanogaster* (http://flybase.org), this database was included due to its high number of identified sequences for soluble binding proteins; *A. mellifera* and *N. vitripennis* (http://hymenopteragenome.org), as taxonomically related species with genomic information and annotated genes of soluble binding proteins; and *Diachasma alloeum* Muesebeck (Hymenoptera: Braconidae); *Fopius arisanus* Sonan (Hymenoptera: Braconidae); *Microplitis demolitor* Wilkinson (Hymenoptera: Braconidae), and *M. mediator* (http://www.insect-genome.com) as the closest related species. Transcript identification and annotation were also analyzed by BLASTn searches on the NCBI databases (https://blast.ncbi.nlm.nih.gov/Blast.cgi?PROGRAM=blastn&PAGE_TYPE=BlastSearch &LINK_LOC=blasthome). The nucleotide sequences of transcripts were translated to protein sequences using the NCBI ORFinder (https://www.ncbi.nlm.nih.gov/orffinder) and checked again (BLASTp) on the database SWISS-PROT (https://www.uniprot.org/blast/). The data analyzed in this study comes from a transcriptome of *D. longicaudata* [41] submitted to NCBI as Sequence Read Archive under the accession number SRP072867. The mentioned Transcriptome Shotgun Assembly project has been deposited at GenBank under the accession GELG00000000.

Transcript sequences and phylogenetic analyses

A phylogenetic analysis was performed using the Bayesian Inference (BI) method and a Conserved Domain Analysis, based on the amino acid sequences (open reading frames) of selected transcripts (S1 Table). The orthologous protein sequences from the genomes and transcriptomes of the following species were used in the analysis: *A. mellifera*; *N. vitripennis*; *F. arisanus*; *D. alloeum*, and *M. demolitor*. The protein sequence alignments were performed using Clustal Ω (https://www.ebi.ac.uk/Tools/msa/clustalo/) and Pfam database [42] and Bioedit to edit the alignments [43]. The domain analysis was performed using the EMBO-InterPro Scan (https://www.ebi.ac.uk/interpro/) and SignalP-5.0 Server (http://www.cbs.dtu.dk/services/SignalP/). The XML files necessary for the BI analysis were generated by using Beauti v1.8.3 [44]. The amino acid substitution model used in the analyses was LG model G+I (5 categories) for CSPs and WAG model+G+I (5 categories) for OBPs and NPC2-like proteins (determined by Mega v6), and the Yule Speciation Model was used in all analyses [45]. Beast v1.8.4 [44] on CIPRES Science Gateway server [46] was used for the BI analyses. Two independent chains were made

under the same conditions until the convergence was achieved, where the effective sample size value was > 200, and determined with Tracer v.1.6.0. Each run produced 100 million trees from a random tree. Both runs were combined using LogCombiner v1.83 discarding the first 10% of each run. The tree with the maximum credibility of the clade was obtained with TreeAnnotator v1.8.3, visualized, and edited with FigTree v1.4.2 [44]. Finally, the outgroup of each sub-clade was defined as those sequences belonging to the evolutionarily most distant taxa: *A. mellifera* or *N. vitripennis* depending on each sub-clade.

RT-PCR assay

To evaluate the presence of expression of the selected transcripts (S1 Table) and to perform RT-PCR reactions, cDNA samples from each tissue: whole body (without antennae) and antennae (for males and females), and ovipositor (only for females) were used as template (2 μl of a 1:10 dilution). The quality of the synthesized cDNA was checked by using elongation factor 1-alpha (EF1-α) as a positive control (S1 Table). All primers were designed by using Primer3web (http://bioinfo.ut.ee/ primer3/) and manufactured by Invitrogen® (Carlsbad, CA, USA). Taq DNA polymerase Kit (Taq Pegasus PB-L®) was used for RT-PCR reactions, according to the manufacturer's specifications, and at the following temperature-cycling parameters: 95˚C, 5 min (1 cycle); 94˚C, 15 s; 58˚C, 15 s; 72˚C, 20 s (35 cycles); 72˚C, 10 min (1 cycle). PCR amplicons were run in 1% w/v agarose gel electrophoresis and visualized by ethidium bromide staining.

Quantitative real-time PCR (qPCR)

Selected transcripts identified *in silico* as potential soluble binding proteins (S1 Table) were analyzed by qPCR to characterize their expression levels. The cDNA samples from female body (without antennae) and from antennae of females (five biological replicates for each of the treatments) were used in the analysis.

qPCR reactions were performed in a Light Cycler 96 (Roche®) and each reaction consisted of a total volume of 10 μl, containing 5 μl of Fast Start Essential DNA Green Master (Roche®), 0.2 μl (10 μM) of each forward and reverse primers, 2.6 μl of dH2O, and 2 μl of cDNA template (a 1:10 dilution of a solution of ~500 ng / μl). The cycling parameter was 95˚C for 5 min, followed by 40 cycles at 95˚C for 10 s and 60˚C for 45 s, ending with a melting curve product amplification. All qPCR experiments were performed according to previously defined parameters [41]. EF1-α and β actin were used as internal reference genes (S1 Table), previously used in this species [41]. The stability and suitability of these reference genes were evaluated with BestKeeper, Normfinder, Genorm, and the comparative delta-Ct method software tools [47, 48]. The normalized relative quantity (NRQ) was calculated for each gene of interest (GOI) following the formulas in [49], and statistical analysis was performed over the Log2 (NRQ) according to [50].

PCR amplicons from the analyzed transcripts were purified and sequenced (forward and reverse primer) by an automatic sequencer—capillary electrophoresis (SIGYSA, IABIMO, CONICET-INTA, Buenos Aires, Argentina) to confirm their nucleotide sequence and univocal identity.

Synthesis of dsRNA and delivery method

The selection of candidate transcripts to be analyzed by RNA interference (RNAi) [51] was based on the phylogenetic analyses performed in the present study and previous reports on taxonomically related species (Hymenoptera: Braconidae) [31, 52, 53]. For the RNAi assay, a coding fragment of each selected gene was amplified by RT-PCR using gene-specific primers

(S1 Table). The products obtained were used as a template for the synthesis of dsRNA by using the RNA Pol. T7 Kit (Thermo Fisher Scientific®, MEGAscript™ RNAi Kit). The dsRNA was resuspended and provided to the insects in sterile tap water to avoid the osmotic shock. Blue food dye Erioglaucine (E133, Merck®, Darmstadt, Germany) was used in the water to identify the insects that consumed the dsRNA by assessing the presence of light blue color in their abdomens. We established a dose of 0.005% w/v to observe the color effect in the treated insects, although higher doses are harmless to insects [54]. The insects (naïve females), previously starved for 48 h, had access to a colored water solution of 20 ng / μl dsRNA for 48 h. Each insect ingested ~ 100 ng of dsRNA (~ 5 μl of solution) and fed on honey *ad libitum*, adapted from [55–57]. The control group received the same treatment, but the dsRNA was specific to the enhanced green fluorescent protein gene (eGFP), absent in insect species genomes and previously used as a control dsRNA of RNAi experiments in other braconid wasps [57].

After the behavioral experiment (see below), the decrease in mRNA levels of target transcripts was assessed by qPCR. The RNA and cDNA samples were obtained from females randomly selected for each treatment (2 h after the behavioral assay) using the above-mentioned protocols. Each sample consisted of the whole body of five pooled females. The qPCR was performed following the methods described above.

Joint silencing was performed for OBPs 9, 10, 11, and 12 proteins, given their high similarity at the nucleotide sequence level (S1A Fig) and because individual silencing was not obtained in preliminary assays. However, the level of expression of each of these transcripts was analyzed by qPCR, since this technique has a higher level of accuracy at the sequence level than the RNAi, as previously described by [58]. For this purpose, two different dsRNAs (both inside the coding region: 70–469 pb) were used: ds(OBP9-12)a from 93 to 346 pb and ds(OBP9-12)b from 189 to 468 pb (S1A Fig).

Foraging behavior and survival assays

The performance of RNAi-silenced females (7–10-day-old naïve females) was evaluated by behavioral assays under laboratory conditions. The experiment was conducted in groups of five *D. longicaudata* females (n = 20 groups tested per treatment). The grouping strategy to evaluate the oviposition behavior of females was implemented because the presence of conspecifics increases parasitic activity [59]. The dsRNA was delivered in dyed water for 48 h and replaced with tap water 48 h before the assay. The behavioral assays were carried out 96 h after the application of the dsRNA. The experimental design was adapted from [55, 59] and defined after preliminary assays. For the assay, five females were placed in a small glass container (5.5 cm in diameter, 13 cm high) covered with a 6 cm Petri dish, placed inside a bigger cylindrical glass container (20 cm in diameter and 30 cm in height) closed at the top with a voile cloth, forming the experimental arena. A thin thread connected to the Petri dish made it possible to release the females from outside the arena with minimal disturbance. The females remained in the smallest container for 24 h before the assays for habituation. During the assay, 250 L3 larvae of *A. fraterculus* were offered in an oviposition unit (OU) that consisted of a Petri dish wrapped in voile cloth placed upside down [39]. Each treatment was tested for 25 min. Once the RNAi-silenced and control females were released, two variables were recorded: i) the number of females foraging on the OU every one minute; and ii) the latency for the first female to visit the OU. After the assay, the larvae from each replicate were placed in 200 mL jars with vermiculite as pupation substrate and kept under controlled conditions (25 ± 1˚C; 65 ± 5% R. H.) to record the number of emerged parasitoids. In all cases, the conditions detailed previously were adapted from [60]. In addition, after the behavioral assays, female survival was

recorded (n = 150 females) on RNAi-silenced and control females based on the protocol and variables described by Viscarret *et al.* [39]. We registered the following variables: i) mean longevity of the adult female (lifespan of the i female/initial number of females); ii) mean survival by age (lx), (number of female at age x/initial number of females).

Statistical analysis

Data analysis was performed using SPSS Statistics 22.0 software (SPSS Inc., Chicago, IL, USA). A two-tailed Student's t-test [61] was performed on the data for all experiments (qPCR, foraging, and survival assays), and the results are presented as the mean ± SEM. For mean longevity analysis, a Log-rank (Mantel-Cox) test was used [62]. The results were plotted using the Prism GraphPad v6 software (GraphPad Software, Inc. Accessed 10/04/2020; http://www.graphpad.com/faq/viewfaq.cfm?faq=1362).

Results

Identification of soluble binding protein transcripts

The bioinformatic analyses of transcripts identified from the *D. longicaudata* whole-body transcriptome [41] yielded the following unigenes: seven CSPs, with two possible isoforms for CSP 3 (CSPs 10 and CSP 11, S1B Fig); 14 OBPs; and four NPC2-like proteins. Detailed information on each identified transcript is listed and categorized in Table 1.

Sequence and phylogenetic analysis

Phylogenetic trees for CSP, OBP, and NPC2-like proteins (Figs 1–3 respectively) showed that each protein sequence of *D. longicaudata* was clustered with the proteins of other closely related hymenopteran species. The phylogenetic analyses revealed that all classes of soluble binding proteins (CSP, OBP, and NPC2-like) analyzed here were significantly different from each other within *D. longicaudata* (posterior values > 0.5, BI analysis). In contrast, homologous soluble binding proteins among species shared a highly similar amino acid sequence and were associated within the same clade with high posterior values support (Figs 1–3).

Amino acid sequence analysis of the soluble binding protein identified in *D. longicaudata* showed a percentage of identity ranging from 19% to 54% (30% on average) in the case of CSPs (S2A Fig). OBP protein sequences shared a percentage of identity between 15% and 90% (23% on average) (S2B Fig), and NPC2-like proteins shared between 23% and 32% (26% on average) of their amino acid sequences (S2C Fig). Regarding the number of conserved cysteines in the sequences, all members of the CSPs family possess the four typical cysteines, characteristic of this group. For OBPs members, only the Classic OBP motif (six conserved cysteines) was found. In several cases (OBPs 3, 5, 6, 8, 9, 10, 11, 12, and 14), an additional conserved cysteine was observed, but inside the signal peptide (~ 1–21 aa) and not as part of an α-helix. All the identified NPC2-like proteins had seven conserved cysteines in their amino acid sequences.

Expression patterns of soluble binding protein transcripts

RT-PCR results showed that all soluble binding protein transcripts (CSP, OBP, and NPC2-like) were detected in all tissues analyzed, antennae and the whole body (without antennae) (both sexes) and ovipositor (only females) (S3–S12 Figs). Sequencing by capillary electrophoresis was used to confirm the identity of the transcripts analyzed by RT-PCR and qPCR (S13 Fig). qPCR analysis was performed only for females, because the main objective of the

Table 1. Soluble binding proteins identified in a whole body transcriptome of *D. longicaudata*.

Gene name	*D. longicaudata* transcriptome database (best tBLASTn hit)					UniprotKB/SwissProt database (best BLASTp hit)				
	Accession Number	Score	E-value	ID query	Species	Gene subject	ID sequence	Score	E-value	Ident
CSP1	GELG01006173.1	77.8	7E-19	DQ855486	*A. mellifera*	PebIII_2 /CSP (*F. arisanus*)	A0A0C9RC91	215	2.40E-20	40 %
CSP2	GELG01043217.1	93.6	1E-25	NP_726402.1	*D. melanogaster*	PebIII_4/CSP (*F. arisanus*)	A0A0C9Q9U6	289	5.00E-35	98.0%
CSP3	GELG01013729.1	109	7E-31	NP_611990.1	*D. melanogaster*	PebIII_9/CSP (*F. arisanus*)	A0A0C9R9K1	283	2.3E-30	48 %
CSP4‡	GELG01000290.1	141	2E-40	DQ855484	*A. mellifera*	transcriptome assembly error (equal sequence than CSP5)	-	-	-	-
CSP5	GELG01000294.1	141	7E-43	DQ855484	*A. mellifera*	PebIII_1 /CSP (*F. arisanus*)	A0A0C9QFN9	470	2.4E-58	67 %
CSP6	GELG01007750.1	142	2E-43	DQ855487	*A. mellifera*	PebIII_6/CSP (*F. arisanus*)	A0A0C9RRW4	568	2.2E-73	83.3%
CSP7&	GELG01001790.1	166	2E-52	NP_611990.1	*D. melanogaster*	Chemosensory protein 1 (*Bactrocera dorsalis*)	A0A034W0K7	552	3.8E-71	91.4%
CSP8	GELG01048086.1	79.7	2E-19	XP_011307929.1	*F. arisanus*	PebIII_3/CSP (*F. arisanus*)	A0A0C9R724	429	1.2E-57	95.9%
CSP9	GELG01007729.1	196	1E-64	XP_011296666.1	*F. arisanus*	A10_0/CSP (*F. arisanus*)	A0A0C9RWR5	487	2.3E-61	76.7%
CSP10†	GELG01015394.1	115	2E-33	XP_011305927.1	*F. arisanus*	PebIII_9/CSP (*F. arisanus*)	A0A0C9R9K1	274	1.00E-28	43.9%
CSP11†	GELG01010361.1	114	1E-32	XP_011305927.1	*F. arisanus*	PebIII_9/CSP (*F. arisanus*)	A0A0C9R9K1	286	1.8E-30	43.3%
OBP1	GELG01005963.1	62.4	6E-13	NV10225-PA	*N. vitripennis*	Pbprp1_1/OBP (*F. arisanus*)	A0A0C9RWQ2	507	1.1E-63	65.2%
OBP2	GELG01007924.1	51.6	1E-09	NV12594-PA	*N. vitripennis*	OBP1 (*F. arisanus*)	A0A0C9QKG6	542	5.4E-68	72.8%
OBP3	GELG01007569.1	81.3	5E-20	NV12608-PA	*N. vitripennis*	Obp56d_4 (*F. arisanus*)	A0A0C9RSX5	439	3.2E-53	63.2%
OBP4	GELG01006993.1	117	5E-33	XP_008543434.1	*M. demolitor*	Obp19a_0 (*F. arisanus*)	A0A0C9QRI4	616	4.6E-80	76.0%
OBP5	GELG01007011.1	140	3E-42	XP_008559486.1	*M. demolitor*	Odorant binding protein 3 (*Macrocentrus cingulum*)	A0A221I2K4	381	1.6E-44	53.0%
OBP6	GELG01005241.1	238	3E-79	XP_011304865.1	*F. arisanus*	Pbprp1_2/OBP (*F. arisanus*)	A0A0C9RWT1	683	1.9E-90	89.4%
OBP7	GELG01007880.1	33.9	0.006	NV15819-PA	*N. vitripennis*	SecA_0/OBP (*F. arisanus*)	A0A0C9R7J0	254	2.5E-25	35.6%
OBP8	GELG01002295.1	139	5E-39	XP_008559486.1	*M. demolitor*	Odorant binding protein 10 (*M. mediator*)	G3M0D3	354	2.1E-40	45.0%
OBP9	GELG01001415.1	123	4E-35	XP_011311566.1	*F. arisanus*	Obp56a (*F. arisanus*)	A0A0C9PK74	319	2.8E-35	43.5%
OBP10	GELG01001518.1	157	1E-47	XP_011311566.1	*F. arisanus*	Obp56a (*F. arisanus*)	A0A0C9PK74	410	6.7E-49	64.3%
OBP11	GELG01003729.1	157	7E-47	XP_011311566.1	*F. arisanus*	Obp56a (*F. arisanus*)	A0A0C9PK74	396	5.5E-47	51.2%
OBP12	GELG01001519.1	175	4E-55	XP_011311566.1	*F. arisanus*	Obp56a (*F. arisanus*)	A0A0C9PK74	452	1.7E-55	62.8%
OBP13&	GELG01005757.1	119	2E-33	Obp99a-PA	*D. melanogaster*	General odorant binding protein 99a (*C. capitata*)	W8ASY6	747	3.6E-100	100.0%
OBP14	GELG01031851.1/ GELG01045208.1	88.6	2E-37	GB50936-PA	*A. mellifera*	OBP10 (*A. mellifera*)	Q1W644	529	5.1E-67	80.9%

(*Continued*)

Table 1. (Continued)

OBP15&	GELG01008185.1	144	2E-44	Obp99a-PB	*D. melanogaster*	General odorant binding protein 99a (*C. capitata*)	W8CAL3	802	3.6E-108	100.0%
OBP16&	GELG01008020.1	87.8	2E-22	Obp99a-PA	*D. melanogaster*	General odorant binding protein 99a (*C. capitata*)	W8CD84	777	1.6E-104	100.0%
OBP17	GELG01007052.1	67.8	5E-15	NV12608-PA	*N. vitripennis*	Pbprp1_0/OBP (*F. arisanus*)	A0A0C9PWB3	463	4.2E-57	65.9%
NPC2a	GELG01007456.1	253	6E-83	XP_015119973.1	*D. alloeum*	Protein NPC2 homolog (*Drosophila guanche*)	A0A3B0JF70	377	5E-44	50.3%
NPC2b	GELG01006291.1	255	2E-84	XP_015120673.1	*D. alloeum*	Epididymal secretory protein E1 (*Ooceraea biroi*)	A0A026W6F8	438	4E-48	55.2%
MD-2	GELG01005505.1	249	9E-82	XP_015114239.1	*D. alloeum*	Md-2-related lipid-recognition (*Lasius niger*)	A0A0J7L5K5	479	2E-59	53.5%
ESR16	GELG01007261.1	248	1E-80	XP_015109258.1	*D. alloeum*	Ecdysteroid-regulated 16 kDa protein (*Camponotus floridanus*)	E2AC22	384	7E-45	48.1%

The genes highlighted in gray were excluded from subsequent analysis because they were assembly errors (‡), contamination (&) or possible isoforms (†).
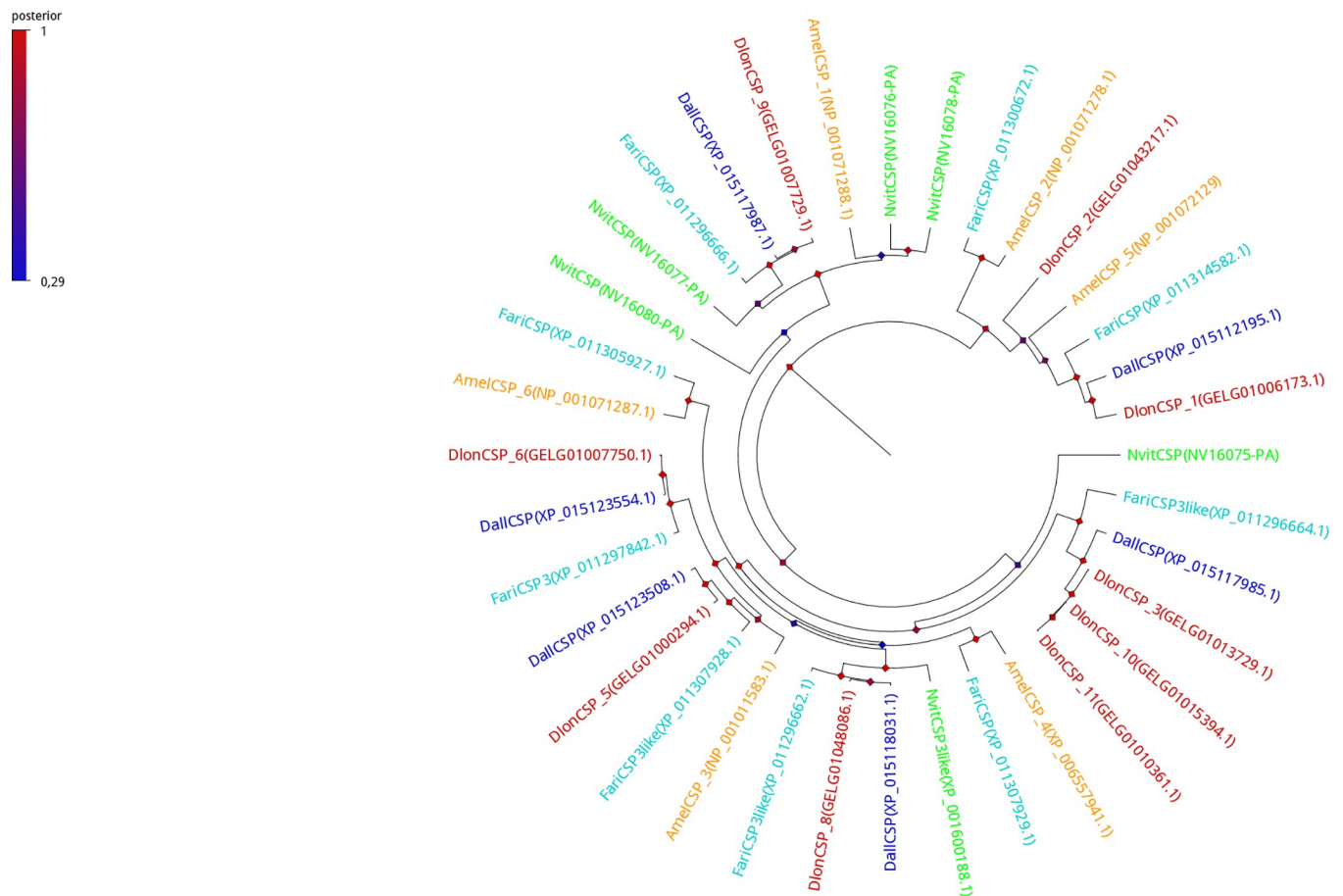
https://doi.org/10.1371/journal.pone.0252765.t001

Fig 1. Phylogenetic tree (Bayesian Inference) of CSP protein sequences from different hymenopteran insects. *A. mellifera* (Amel, yellow); *N. vitripennis* (Nvit, green); *F. arisanus* (Fari, light blue); *D. alloeum* (Dall, blue); and *D. longicaudata* (Dlon, red). Node color indicates posterior values, while red color represents a high credibility node (scale top left).
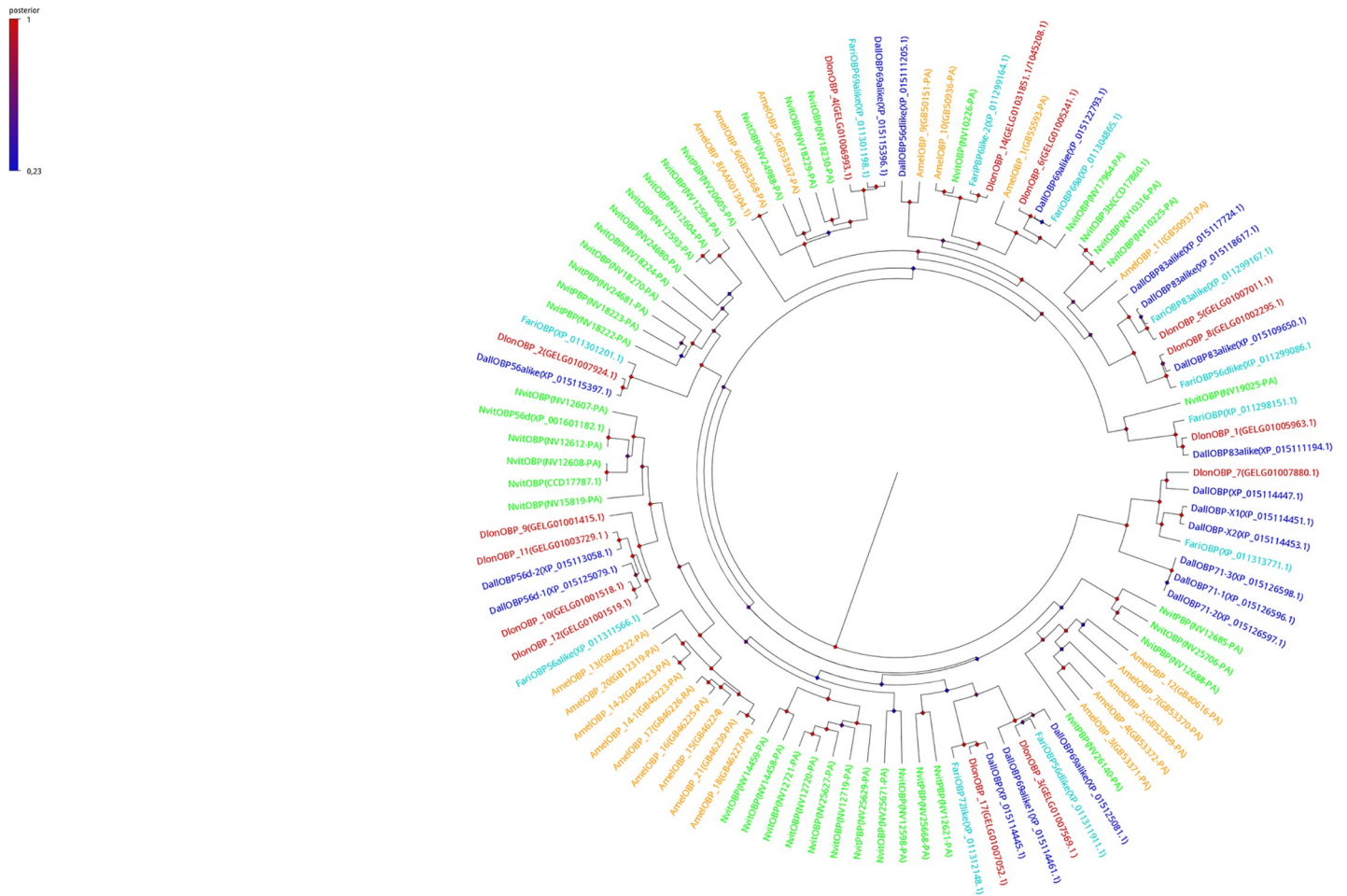
https://doi.org/10.1371/journal.pone.0252765.g001

Fig 2. Phylogenetic tree (Bayesian Inference) of OBP protein sequences from different hymenopteran insects. *A. mellifera* (Amel, yellow); *N. vitripennis* (Nvit, green); *F. arisanus* (Fari, light blue); *D. alloeum* (Dall, blue); and *D. longicaudata* (Dlon, red). Node color indicates posterior values, while red color represents a high credibility node (scale top left).

https://doi.org/10.1371/journal.pone.0252765.g002

present work, is the identification of soluble binding proteins potentially associated to the detection of the host for oviposition.

By means of RT-PCR and sequencing, we identified assembly errors (described as different transcript IDs from the *D. longicaudata* transcriptome matched with the same query sequence or a transcript ID with more than one query sequence) (Table 1). We also detected host contamination, as *Ceratitis capitata* sequences were *in silico* identified for CSP 4 and 7, and OBPs 13, 15, and 16 (Table 1). This type of contamination was confirmed by the absence of PCR amplification in all *D. longicaudata* tissues analyzed (S3–S12 Figs) and *D. longicaudata* genomic DNA. Multiple alignments were performed to compare sequenced PCR amplicons with the transcript assembled sequences to confirm their nucleotide sequence and univocal identity (S13 Fig).

The qPCR analysis performed on the female antenna and body (without antennae) showed that three CSPs were differentially expressed between these tissues. Specifically, CSP 2 and CSP 8 were significantly more highly expressed in female antenna than in the body (p = 0.036 and p = 0.044, respectively). Conversely, CSP 1 was significantly more highly expressed in the body (without antennae) in comparison to antenna (p = 0.040) (Fig 4A). In addition, nine OBPs were
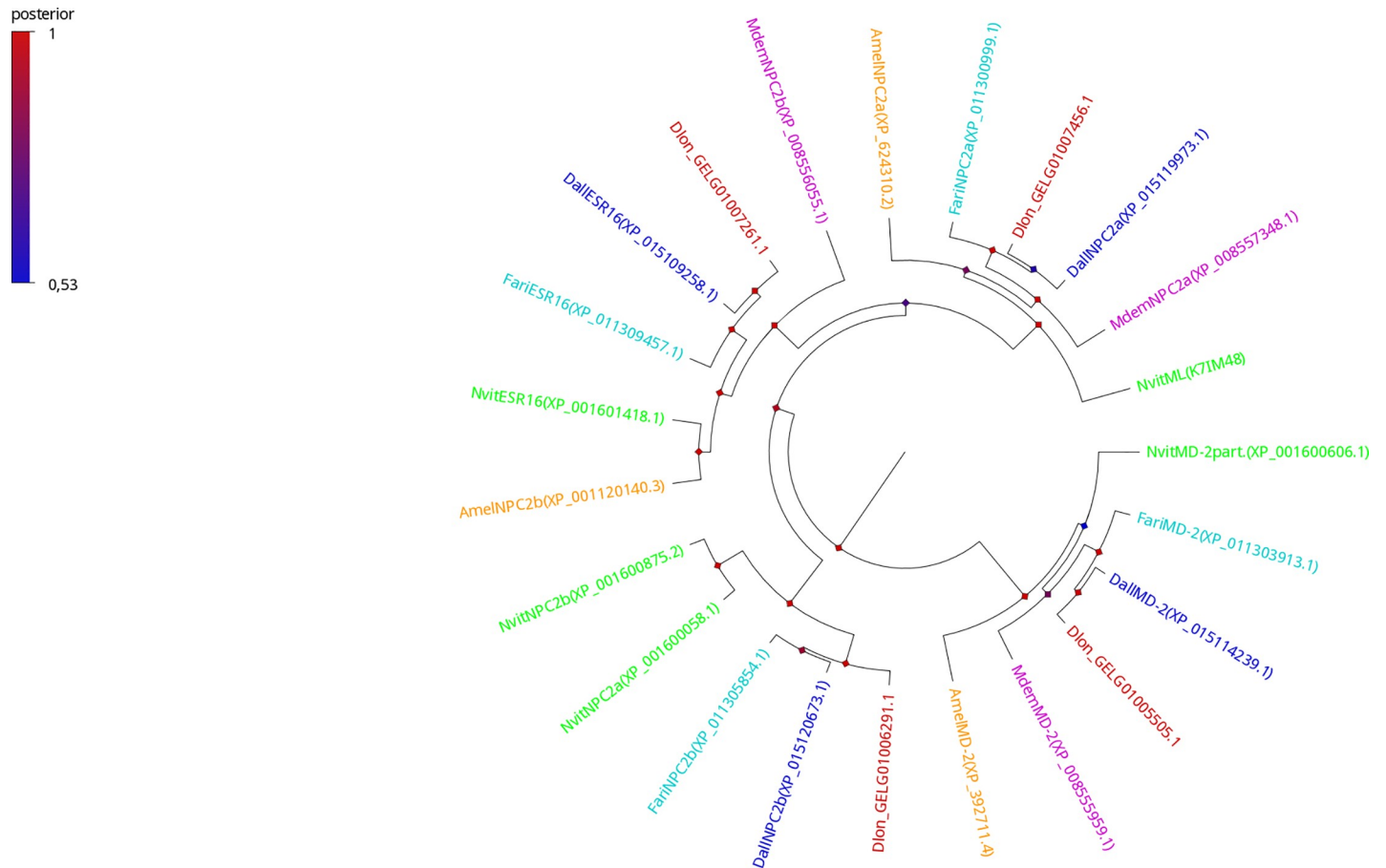
Fig 3. Phylogenetic tree (Bayesian Inference) of NPC2-like protein sequences from different hymenopteran insects. *A. mellifera* (Amel, yellow); *N. vitripennis* (Nvit, green); *F. arisanus* (Fari, light blue); *D. alloeum* (Dall, blue); *M. demolitor* (Mdem, violet) and *D. longicaudata* (Dlon, red). Node color indicates posterior values, while red color represents a high credibility node (scale top left).

https://doi.org/10.1371/journal.pone.0252765.g003

differentially expressed between these tissues. OBP 2 (p = 0.039), OBP 3 (p = 0.050), OBP 4 (p = 0.00007), OBP 5 (p = 0.002), OBP 6 (p = 0.00009), OBP 9 (p = 0.011), OBP 10 (p = 0.011), and OBP 11 (p = 0.043) showed an over-expression in female antenna in comparison to the whole body (without antennae). The opposite pattern was detected for OBP 12 (p = 0.010) (Fig 4B). Regarding NPC2-like transcripts, NPC2b was significantly highly expressed in the female antenna relative to the whole body (without antennae) (p = 0.025) (Fig 4C).

RNAi assays

CSP 3 and OBPs 7, 9, 10, 11, and 12 were selected for the RNAi analysis based on the phylogenetic analyses performed in the present study and previous reports on taxonomically related species. The RNAi effect (the expected decrease in the transcription of silenced genes), evaluated by qPCR of RNAi-silenced females, showed that CSP 3 (p = 0.046) and OBP 7 (p = 0.035) were significantly silenced in comparison to the control groups (Fig 5). Using the RNA interference ds(OBP9-12)a, OBPs 9 and 12 were significantly silenced (n = 5; p = 0.01 and p = 0.004, respectively). Although OBPs 10 and 11 were not significantly affected after the RNAi, their expression levels decreased (p = 0.111 and p = 0.058, respectively) (Fig 5). Conversely, using ds(OBP9-12)b, only OBP 10 was significantly silenced (p = 0.016), and OBP 9,
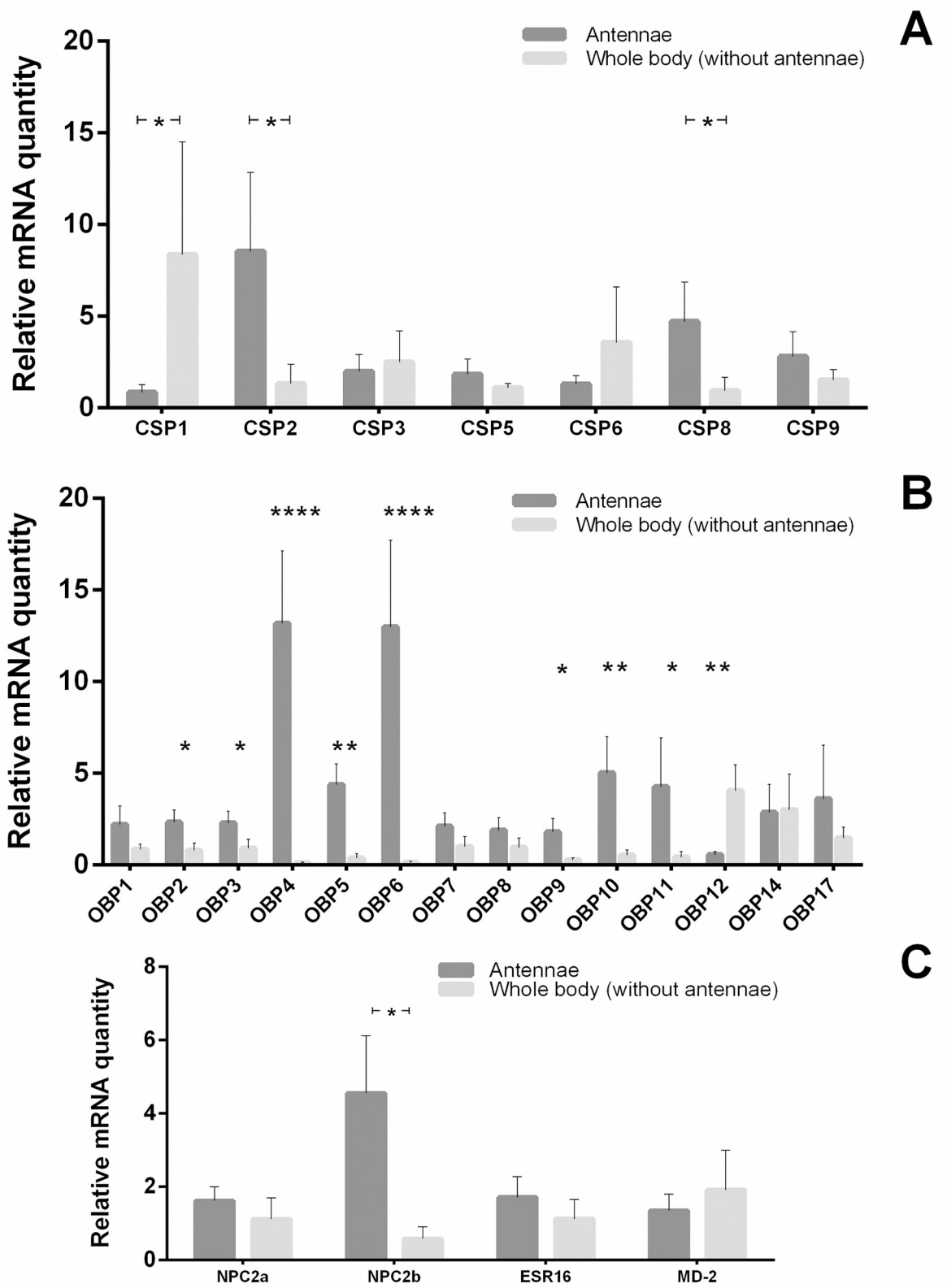
Fig 4. Expression levels of CSPs (A), OBPs (B), and NPC2-like (C) in *D. longicaudata* female tissues by qPCR. The relative expression level (NRQ) is indicated as mean ± SEM. The tissues analyzed were as follows: female whole body (5 female bodies without antennae) and female antenna (the antennae of 30 females per sample). The asterisk (*) represents significant differences (n = 5 samples; * $p < 0.05$, ** $p < 0.01$, **** $p < 0.0001$, two-tailed *t-test*) among the tissues.

11, and 12 decreased their expression levels by 50, 80, and 30%, respectively, although they were not significantly different from the control treatment ($p = 0.125$, $p = 0.110$, and $p = 0.191$, respectively) (Fig 5).

Behavioral assays on RNAi-silenced females

Foraging behavior and survival of adult females were evaluated for silenced and non-silenced (control) adult females. For dsCSP 3 silenced females, the number of females foraging on the OUs, the latency for the first female to visit the OU, and the number of emerged parasitoids were significantly affected in comparison to the control treatments (dsGFP). The foraging behavior and the number of emerged parasitoids (from fly larvae used in the assays) decreased their values in the case of silenced females ($p = 0.012$ and $p = 0.015$, respectively). Conversely, the latency had increased values in this group ($p = 0.019$) (Fig 6A–6C). Silencing of OBPs 9–12 (using two different dsRNAs) was also associated with females' foraging performance. RNA interference ds(OBP9-12)a decreased the foraging behavior and the number of emerged parasitoids ($p = 0.020$ and $p = 0.035$, respectively), but the latency increased ($p = 0.049$). Using ds(OBP9-12)b showed a decrease in foraging behavior and emerged parasitoids ($p = 0.046$ and $p = 0.044$, respectively), but an increased latency ($p = 0.018$). The treatment of the OBP 7 showed no significant difference for the three recorded variables (number of females foraging on the OU, the latency for the first female to visit the OU, and the number of emerged parasitoids) ($p = 0.298$, $p = 0.318$ and $p = 0.439$, respectively).

After the behavioral assays, the survival of RNAi-silenced females was recorded. CSP 3-silenced females showed an increased mean longevity and mean survival by age ($p < 0.0001$
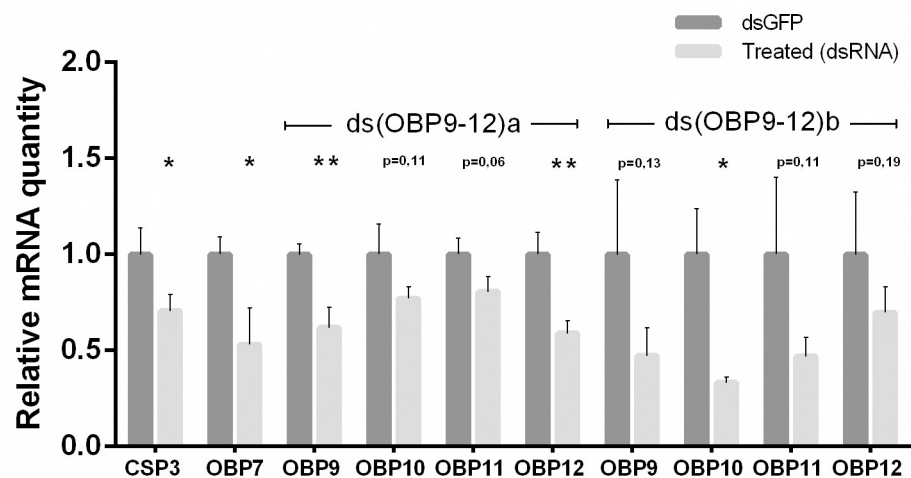

Fig 5. Transcript expression levels in response to dsRNA treatment measured by qPCR. The normalized relative quantity (NRQ), represented as fold change relative to controls, is indicated as mean ± SEM (n = 5 female whole-body per sample). The asterisk (*) represents significant differences (n = 5; * $p < 0.05$ two-tailed *t-test*) among target gene-specific dsRNA and control dsRNA (eGFP).
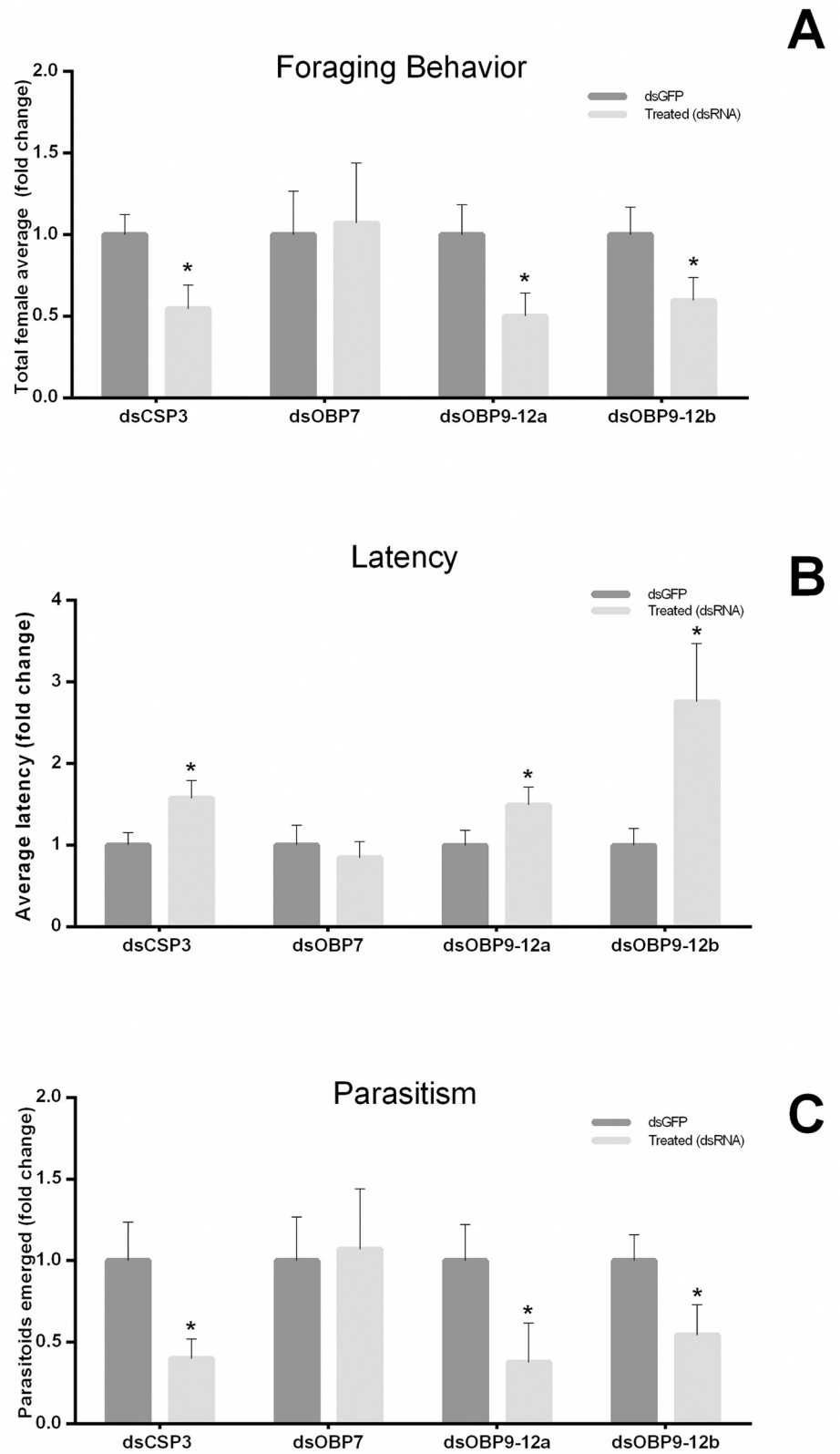
Fig 6. *In vivo* performance of females (previously silenced by CSP 3, OBPs 7, 9, 10, 11, and 12) by behavioral assays: (A) Foraging behavior; (B) Latency time and (C) Parasitism rate. The asterisk (*) represents significant differences (n = 14 all treatments and n = 7 for OBP7; * p < 0.05 two-tailed *t*-test) among target-gene-specific dsRNA and control dsRNA (eGFP).

https://doi.org/10.1371/journal.pone.0252765.g006

and p < 0.0001, respectively) (Fig 7A and 7B), as did females treated with ds(OBP9-12)a (p = 0.020 and p = 0.016, respectively) (Fig 7E and 7F). The treatment with ds(OBP9-12)b triggered a decrease in survival by age only in OBP 10-silenced females (p = 0.034), but there were no changes in the mean longevity (p = 0.313) (Fig 7G and 7H). OBP 7 showed no significant difference in mean longevity and mean survival by age (p = 0.229 and p = 0.286, respectively) (Fig 7C and 7D).

Discussion

This study reports the identification, a first sequence characterization, and the behavioral evaluation of soluble binding proteins in *D. longicaudata*. The number of sequences identified here were similar to that of other hymenopteran species: *A. mellifera*, six CSPs, 21 OBPs and two NPC2-like [19, 63]; *N. vitripennis*, nine CSPs, 90 OBPs and four NPC2-like [64]; *M. mediator*, three CSPs, 20 OBPs and two NPC2-like [33, 65]; *F. arisanus*, nine CSPs, 11 OBPs and four NPC2-like [66] and *D. alloeum*, nine CSPs, 15 OBPs and four NPC2-like [67]. However, the identified soluble binding proteins do not match the number of transcripts identified in a transcriptome of pooled tissues (antenna, head, thorax, abdomen, and legs) of *D. longicaudata*, which reported 69 CSPs and 43 OBPs [68]. The reason for such differences might be related to the fact that we based our screening on a transcriptome obtained from the whole body of the wasp, which might have reduced the representation of genes expressed mainly in structures with a high content of cuticle, such as antenna. In fact, only classic OBPs were identified in this work, whereas OBPs like ABPXs, CRLBP, and D7 (which are mainly expressed in olfactory and gustatory structures such as antenna and insect mouthparts) [69, 70] were not detected.

Gene expression profile analyzed by RT-PCR on male and female tissues (antennae, rest of the body, and ovipositor) showed similarities for all soluble binding proteins tested on all the tissues analyzed. However, qPCR analysis on the female antenna and the rest of the body showed that three CSPs, nine OBPs, and one NPC2-like transcripts were differentially expressed between these tissues. Transcripts with a high expression in the female antenna (CSPs 2 and 8, OBPs 2, 3, 4, 5, 6, 9, 10, and 11, and NPC2b) would be potentially related to physiological processes such as host-seeking, feeding, and mating. On the other hand, those transcripts highly expressed in the body (CSP 1 and OBP 12) are potentially related to other physiological processes such as lipid homeostasis and reproduction [1, 4, 5]. Concerning NPC2-like proteins, this particular sub-family (with 7 cysteines conserved in the protein sequence) was found to be mostly associated with structures with chemosensory functions in other insects [4, 17].

The results of the behavioral and qPCR analysis support the hypothesis that OBPs 9–11 are involved in female foraging behavior. Besides, behavioral and qPCR assays support the hypothesis that OBP 12 is involved in physiological processes, directly or indirectly related to longevity. In addition, the hypothesis that CSP 3 and OBP 12 are related to foraging behavior was only supported by the behavioral assays. Regarding CSP 3, its orthologous sequence in *M. mediator* (MmedCSP1) showed high expression in adult antennae [71]. Moreover, MmedCSP3 is expressed exclusively in a type 2 basiconica sensillum [71], and the neurons associated with this sensillum have shown high responses to volatile plant compounds [72]. About OBPs 9–12, its orthologous sequences of the parasitoid wasp *Chouioia cunea*
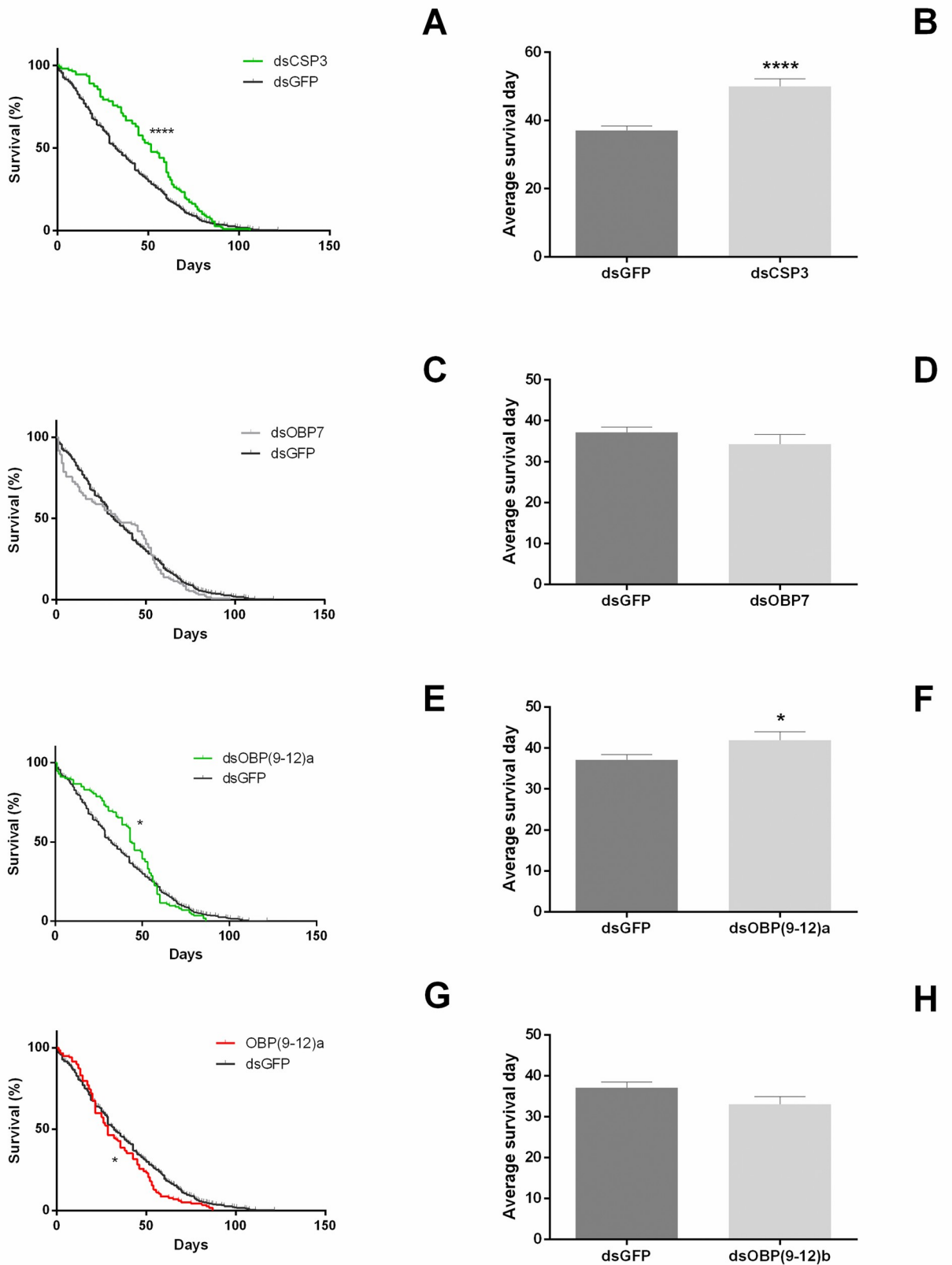
Fig 7. *In vivo* performance of females (previously silenced by CSP 3, OBPs 7, 9, 10, 11, and 12) by behavioral trials: survival analysis measured as mean longevity of the adult females (A, C, E, and G) and survival analysis measured as mean survival by age (B, D, F, and H). The asterisk (*) represents significant differences among target gene-specific dsRNA and control dsRNA (eGFP), for survival analysis (n = 150; * p < 0.05 and **** p < 0.0001 two-tailed *t*-test) and mean longevity analysis (n = 150; * p < 0.05 and **** p < 0.0001 Mantel-Cox).

(CcunOBP2, 9, and 10) are highly expressed in adult antennae and head [73]. In another wasp species, *Sclerodermus* sp, its orthologous sequences (SspOBP4, 5, and 6) are mostly expressed in female antennae [53]. Moreover, it is interesting that an orthologous sequence of this cluster of proteins in *Phormia regina* (PregOBP56a) is believed to solubilize fatty acids during feeding, and subsequently, it helps to deliver the fatty acids to the midgut [22].

Our results suggest that CSP 3 and OBPs 9–11, but more likely OBP 12, are potentially associated with the regulation of mean longevity of the adult females. This could indicate that the transcriptional gene silencing of these soluble binding proteins (associated with an increase in longevity) could be related to energy-saving pathways, as protein translation process represents one of the most expensive stages in energetic terms, in comparison to other physiological processes [74, 75]. Furthermore, these proteins were found at very high concentrations (between 10–20 mM) in different tissues of other insect species [6]. However, silencing chemosensory-related transcripts do not always affect longevity. Such is the case of RproOBP27 in *Rhodnius prolixus* [76] or OBP 7 in this study, which could indicate that this phenomenon is specific to certain soluble binding proteins. One possible explanation is that some of these proteins act as lipid carriers in some insect species [22].

Several studies in *D. melanogaster* and *Caenorabditis elegans* indicate that there is a delicate balance between longevity and lipid homeostasis [*e.g.* 77]. Furthermore, this balance could be affected by different biological processes, such as an increase in lipid transport and lipase activity in the midgut, acting on lipid homeostasis and increasing the average longevity of individuals [78]. Differences observed in the mean longevity of adult females between ds(OBP9-12)a and ds(OBP9-12)b can be associated with similar processes (transport of fatty acids), carried out by the same or different genes (*e.g.* OBP 12), but in different tissues. We take as reference *D. melanogaster* and *C. elegans*, where an increase in the lipid concentration in different tissues, such as fat body and midgut, has an antagonistic effect on longevity [77–80]. A second hypothesis could be that this phenomenon is associated, on the one hand, with an off-target effect, related to energy saving for certain proteins, and on the other, to a specific effect only for OBP 12, the only protein of this group that showed a high expression in the rest of the body. To confirm these hypotheses, gene expression should be evaluated in different tissues and periods and under different starvation conditions.

The results presented in this work are in agreement with previous studies, which indicate that soluble binding proteins are involved in different physiological processes and behaviors, such as host-seeking and mean longevity [4, 81]. There is an increasing interest in the development of sustainable and innovative strategies to control insect pest species using the information generated of chemosensory genes [5, 28]. However, soluble binding proteins (mainly for OBPs) are encoded by genes subjected to rapid evolution rates [82–84], and this should be considered in studies of these genes as potential targets associated with biological control. Moreover, this rapid evolution, in some species, results in clade expansions (mainly for OBPs), facilitating the development of species-specific strategies [85, 86].

The study of soluble binding proteins also evidenced the complexity of the underlying molecular mechanisms, since several roles have been described for their orthologous sequences, either in the same or different species, such as recognition and solubilization of ligands; concentration of chemical elements in the sensillum lymph and/or ligand protection; removal or deactivation of odorants after receptor stimulation and ligand desorption [87–91].

Furthermore, recent studies in *D. melanogaster* have demonstrated that ORs can be activated (or even increase the neuronal response) in the absence of OBPs [92, 93], which could indicate that these proteins act more as modulators of specific physiological pathways rather than as indispensable components of such processes [94].

In summary, the present study is a first step in the characterization of the molecular mechanisms associated with the detection of cues related to foraging behavior for oviposition in *D. longicaudata*. The identification of receptors and other molecules involved in chemosensing and the associated volatile compounds may contribute to improving our knowledge of underlying biochemical pathways of this complex trait. In addition, this information will support future developments of attractant baits to monitor the parasitoid in the field and, therefore, improve the efficiency of the biological control strategy against fruit fly species.

Supporting information

S1 Fig. Multiple nucleotide sequence alignment of (A) *D. longicaudata* OBP 9 to 12 nucleotide sequence alignment. Both start and stop codons are highlighted in red (~45/70-470). (B) *D. longicaudata* CSP 3, 10, and 11 nucleotide sequence alignment. Both start and stop codons are highlighted in red (~40–410). Alignments were performed by Clustal Ω alignment.
(PDF)

S2 Fig. Multiple protein sequence alignment of soluble binding proteins from *D. longicaudata* and closely related species: (A) CSPs, the four conserved cysteine residues are marked in black. (B) OBPs, the six conserved cysteine residues are marked in black. (C) NPC2-like proteins, the seven conserved cysteine residues are marked in black. Alignments were performed by Clustal Ω, only the closer orthologous sequence to the *D. longicaudata* sequences (according to phylogenetic analysis) were used to improve the visualization of conserved regions. Identical and positive amino acids are highlighted in dark gray and light gray, respectively. Predicted signal peptides are highlighted in red. *A. mellifera* (Amel); *N. vitripennis* (Nvit); *F. arisanus* (Fari); *D. alloeum* (Dall); *M. demolitor* (Mdem) and *D. longicaudata* (Dlon).
(PDF)

S3 Fig. RT-PCR results of CSPs and NPC2-like proteins in female antennae. From left to right: molecular-weight size marker, CSPs 1–9, NPC2a, NPC2b, ESR16 and MD-2.
(TIF)

S4 Fig. RT-PCR results of OBPs in female antenna. From left to right: molecular-weight size marker, OBPs 1–17.
(TIF)

S5 Fig. RT-PCR results of CSPs and NPC2-like proteins in female body (without antennae). From left to right: molecular-weight size marker, CSPs 1–9 and NPC2a, NPC2b, ESR16, and MD-2.
(TIF)

S6 Fig. RT-PCR results of OBPs in female body (without antennae). From left to right: molecular-weight size marker, OBPs 1–17.
(TIF)

S7 Fig. RT-PCR results of CSPs and NPC2-like proteins in male antenna. From left to right: molecular-weight size marker, CPSs 1–9 and NPC2a, NPC2b, ESR16 and MD-2.
(TIF)

S8 Fig. RT-PCR results of OBPs in male antenna. From left to right: molecular-weight size marker, OBPs 1–17.
(TIF)

S9 Fig. RT-PCR results of CSPs and NPC2-like in male body (without antennae). From left to right: molecular-weight size marker, CSPs 1–9 and NPC2a, NPC2b, ESR16 and MD-2.
(TIF)

S10 Fig. RT-PCR results of OBPs male body (without antennae). From left to right: molecular-weight size marker, OBPs_ from left to right MW, OBPs 1–17.
(TIF)

S11 Fig. RT-PCR results of CSPs and NPC2-like in ovipositor. From left to right: molecular-weight size marker, CSPs 1–9 and NPC2a, NPC2b, ESR16 and MD-2.
(TIF)

S12 Fig. RT-PCR results of OBPs in ovipositor. From left to right: molecular-weight size marker, OBPs 1–17.
(TIF)

S13 Fig. Nucleotide sequence alignments of sequenced PCR amplicons (forward and reverse sequences) and assembled transcripts (obtained from the *D. longicaudata* transcriptome) for the selected genes.
(PDF)

S14 Fig. Potential contamination tested on genomic DNA of *D. longicaudata*. From left to right: molecular-weight size marker, negative control, β Actin as a positive control, CSPs 4 and 7, and OBPs 13, 15, and 16.
(TIF)

S1 Table. Sequence of primers used for RT-PCR, qPCR, and RNA interference.
(XLS)

Acknowledgments

Author Contributions

Conceptualization: Juan P. Wulff, Diego F. Segura, Francisco Devescovi, Silvia B. Lanzavecchia.

Data curation: Juan P. Wulff.

Formal analysis: Juan P. Wulff, Diego F. Segura, Francisco Devescovi, Silvia B. Lanzavecchia.

Funding acquisition: Juan P. Wulff, Diego F. Segura, Silvia B. Lanzavecchia.

Investigation: Juan P. Wulff, Diego F. Segura, Francisco Devescovi, Irina Muntaabski, Fabian H. Milla, Silvia B. Lanzavecchia.

Methodology: Juan P. Wulff, Diego F. Segura, Francisco Devescovi, Alejandra C. Scannapieco, Silvia B. Lanzavecchia.

Project administration: Silvia B. Lanzavecchia.

Resources: Juan P. Wulff, Diego F. Segura, Silvia B. Lanzavecchia.

Supervision: Diego F. Segura, Silvia B. Lanzavecchia.

Visualization: Juan P. Wulff.

Writing – original draft: Juan P. Wulff.

Writing – review & editing: Juan P. Wulff, Diego F. Segura, Francisco Devescovi, Alejandra C. Scannapieco, Jorge L. Cladera, Silvia B. Lanzavecchia.

References

1. Wicher D, Marion-Poll F. Function and Regulation of Chemoreceptors [Internet]. Frontiers Media SA; 2019. Available from: https://books.google.com.ar/books?id=RvWGDwAAQBAJ

2. He P.; Chen G. L.; Li S.; Wang J.; Ma Y. F.; Pan Y. F.; et al., Evolution and functional analysis of odorant-binding proteins in three rice planthoppers: Nilaparvata lugens, Sogatella furcifera, and Laodelphax striatellus. Pest Manag Sci 2019, 75, 1606–1620. https://doi.org/10.1002/ps.5277 PMID: 30515974

3. Vogt RG, Riddiford LM. Pheromone binding and inactivation by moth antennae. Nature. 1981; 293 (5828):161–3. https://doi.org/10.1038/293161a0 PMID: 18074618

4. Pelosi P, Iovinella I, Felicioli A, Dani FR. Soluble proteins of chemical communication: an overview across arthropods. Front Physiol. 2014; 5:320. https://doi.org/10.3389/fphys.2014.00320 PMID: 25221516

5. Leal WS. Odorant reception in insects: roles of receptors, binding proteins, and degrading enzymes. Annu Rev Entomol. 2013; 58:373–91. https://doi.org/10.1146/annurev-ento-120811-153635 PMID: 23020622

6. Vogt RG. The Molecular Basis of Pheromone Reception: Its Influence on Behavior. In: Prestwich GD, Blomquist GJ, editors. Pheromone Biochemistry [Internet]. Academic Press; 1987. p. 385–431.

7. Tegoni M, Campanacci V, Cambillau C. Structural aspects of sexual attraction and chemical communication in insects. Trends Biochem Sci. 2004; 29(5):257–64. https://doi.org/10.1016/j.tibs.2004.03.003 PMID: 15130562

8. Zhu J, Iovinella I, Dani FR, Pelosi P, Wang G. Chemosensory Proteins: A Versatile Binding Family BT —Olfactory Concepts of Insect Control—Alternative to insecticides: Volume 2. In: Picimbon J-F, editor. Cham: Springer International Publishing; 2019. p. 147–69. Available from: https://doi.org/10.1007/978-3-030-05165-5_6

9. McKenna MP, Hekmat-Scafe DS, Gaines P, Carlson JR. Putative Drosophila pheromone-binding proteins expressed in a subregion of the olfactory system. J Biol Chem. 1994; 269(23):16340–7. PMID: 8206941

10. Jacquin-Joly E, Vogt RG, François M-C, Nagnan-Le Meillour P. Functional and expression pattern analysis of chemosensory proteins expressed in antennae and pheromonal gland of Mamestra brassicae. Chem Senses. 2001; 26(7):833–44. https://doi.org/10.1093/chemse/26.7.833 PMID: 11555479

11. Gu S-H, Wang S-Y, Zhang X-Y, Ji P, Liu J-T, Wang G-R, et al. Functional characterizations of chemosensory proteins of the alfalfa plant bug Adelphocoris lineolatus indicate their involvement in host recognition. PLoS One. 2012; 7(8). https://doi.org/10.1371/journal.pone.0042871 PMID: 22900060

12. Maung K, Jing D, Zhang T, He K, Bai S, Wang Z. Structural characteristics of niemann-pick type C2 proteins in Macrocentrus cingulum and similarities with olfactory proteins in hymenoptera. 2019; 7:296–301.

13. Josek T, Walden KKO, Allan BF, Alleyne M, Robertson HM. A foreleg transcriptome for Ixodes scapularis ticks: candidates for chemoreceptors and binding proteins that might be expressed in the sensory Haller's organ. Ticks Tick Borne Dis. 2018; 9(5):1317–27. https://doi.org/10.1016/j.ttbdis.2018.05.013 PMID: 29886186

14. Xiu C, Xiao Y, Zhang S, Bao H, Liu Z, Zhang Y. Niemann-Pick proteins type C2 are identified as olfactory related genes of Pardosa pseudoannulata by transcriptome and expression profile analysis. Comp Biochem Physiol Part D Genomics Proteomics. 2019; 29:320–9. https://doi.org/10.1016/j.cbd.2019.01.004 PMID: 30669056

15. Zheng Y, Wang S, Peng Y, Lu Z, Shan S, Yang Y, et al. Functional characterization of a Niemann–Pick type C2 protein in the parasitoid wasp Microplitis mediator. Insect Sci. 2018; 25(5):765–77. https://doi.org/10.1111/1744-7917.12473 PMID: 28459128

16. Zhu J, Guo M, Ban L, Song L-M, Liu Y, Pelosi P, et al. Niemann-Pick C2 Proteins: A New Function for an Old Family. Front Physiol [Internet]. 2018; 9(52). https://doi.org/10.3389/fphys.2018.00052 PMID: 29472868

17. Shi X-Z, Zhong X, Yu X-Q. Drosophila melanogaster NPC2 proteins bind bacterial cell wall components and may function in immune signal pathways. Insect Biochem Mol Biol. 2012; 42(8):545–56. https://doi.org/10.1016/j.ibmb.2012.04.002 PMID: 22580186

18. Parmakelis A, Moustaka M, Poulakakis N, Louis C, Slotman MA, Marshall JC, et al. Anopheles immune genes and amino acid sites evolving under the effect of positive selection. PLoS One. 2010; 5(1). https://doi.org/10.1371/journal.pone.0008885 PMID: 20126662

19. Wallberg A, Bunikis I, Pettersson OV, Mosbech M-B, Childers AK, Evans JD, et al. A hybrid de novo genome assembly of the honeybee, Apis mellifera, with chromosome-length scaffolds. BMC Genomics. 2019; 20(1):275. https://doi.org/10.1186/s12864-019-5642-0 PMID: 30961563

20. Findlay GD, Yi X, MacCoss MJ, Swanson WJ. Proteomics reveals novel Drosophila seminal fluid proteins transferred at mating. PLoS Biol. 2008; 6(7). https://doi.org/10.1371/journal.pbio.0060178 PMID: 18666829

21. Danneels EL, Rivers DB, De Graaf DC. Venom proteins of the parasitoid wasp Nasonia vitripennis: recent discovery of an untapped pharmacopee. Toxins (Basel). 2010; 2(4):494–516. https://doi.org/10.3390/toxins2040494 PMID: 22069597

22. Ishida Y, Ishibashi J, Leal WS. Fatty acid solubilizer from the oral disk of the blowfly. PLoS One. 2013; 8 (1). https://doi.org/10.1371/journal.pone.0051779 PMID: 23326317

23. Maleszka J, Foret S, Saint R, Maleszka R. RNAi-induced phenotypes suggest a novel role for a chemosensory protein CSP5 in the development of embryonic integument in the honeybee (Apis mellifera). Dev Genes Evol. 2007; 217(3):189–96. https://doi.org/10.1007/s00427-006-0127-y PMID: 17216269

24. Zhou X-H, Ban L, Iovinella I, Zhao L-J, Gao Q, Felicioli A, et al. Diversity, abundance, and sex-specific expression of chemosensory proteins in the reproductive organs of the locust Locusta migratoria manilensis. Biol Chem. 2012;394.

25. Huang X, Suyama K, Buchanan J, Zhu AJ, Scott MP. A Drosophila model of the Niemann-Pick type C lysosome storage disease: dnpc1a is required for molting and sterol homeostasis. Development. 2005; 132(22):5115–24. https://doi.org/10.1242/dev.02079 PMID: 16221727

26. Fluegel ML, Parker TJ, Pallanck LJ. Mutations of a Drosophila NPC1 gene confer sterol and ecdysone metabolic defects. Genetics. 2006; 172(1):185–96. https://doi.org/10.1534/genetics.105.046565 PMID: 16079224

27. Wang ML, Motamed M, Infante RE, Abi-Mosleh L, Kwon HJ, Brown MS, et al. Identification of surface residues on Niemann-Pick C2 essential for hydrophobic handoff of cholesterol to NPC1 in lysosomes. Cell Metab. 2010; 12(2):166–73. https://doi.org/10.1016/j.cmet.2010.05.016 PMID: 20674861

28. Venthur H, Zhou J-J. Odorant receptors and odorant-binding proteins as insect pest control targets: a comparative analysis. Front Physiol. 2018; 9:1163. https://doi.org/10.3389/fphys.2018.01163 PMID: 30197600

29. Wang Z, Liu Y, Shi M, Huang J, Chen X. Parasitoid wasps as effective biological control agents. J Integr Agric [Internet]. 2019; 18(4):705–15. Available from: http://www.sciencedirect.com/science/article/pii/S2095311918620787

30. Colazza S, Peri E, Salerno G, Conti E. Host Searching by Egg Parasitoids: Exploitation of Host Chemical Cues. In 2010. p. 97–147.

31. Zhang S, Chen L-Z, Gu S-H, Cui J-J, Gao X-W, Zhang Y-J, et al. Binding characterization of recombinant odorant-binding proteins from the parasitic wasp, Microplitis mediator (Hymenoptera: Braconidae). J Chem Ecol. 2011; 37(2):189–94. https://doi.org/10.1007/s10886-010-9902-3 PMID: 21184151

32. Wang Y, Chen Q, Guo J, Li J, Wang J, Wen M, et al. Molecular basis of peripheral olfactory sensing during oviposition in the behavior of the parasitic wasp Anastatus japonicus. Insect Biochem Mol Biol. 2017; 89:58–70. https://doi.org/10.1016/j.ibmb.2017.09.001 PMID: 28912112

33. Wang G-Y, Zhu J-L, Zhou W-W, Liu S, Khairul QM, Ansari NA, et al. Identification and expression analysis of putative chemoreception genes from Cyrtorhinus lividipennis (Hemiptera: Miridae) antennal transcriptome. Sci Rep. 2018; 8(1):1–10. https://doi.org/10.1038/s41598-017-17765-5 PMID: 29311619

34. Yi S-Y, Li D-Z, Zhou C-X, Tang Y-L, Abdelnabby HE, Wang M-Q. Screening behaviorally active compounds based on fluorescence quenching in combination with binding mechanism analyses of SspOBP7, an odorant binding protein from Sclerodermus sp. Int J Biol Macromol. 2018; 107:2667–78. https://doi.org/10.1016/j.ijbiomac.2017.10.149 PMID: 29113892

35. Ovruski SM, Bezdjian LP, Van Nieuwenhove GA, Albornoz-Medina P, Schliserman P. Host preference by Diachasmimorpha longicaudata (Hymneoptera: Braconidae) reared on larvae of Anastrepha fraterculus and Ceratitis capitata (Diptera: Tephritidae). Florida Entomol. 2011; 94(2):195–200.

36. Segura DF, Nussenbaum AL, Viscarret MM, Devescovi F, Bachmann GE, Corley JC, et al. Innate host habitat preference in the parasitoid Diachasmimorpha longicaudata: functional significance and modifications through learning. PLoS One. 2016; 11(3). https://doi.org/10.1371/journal.pone.0152222 PMID: 27007298

37. Segura DF, Viscarret MM, Ovruski SM, Cladera JL. Response of the fruit fly parasitoid Diachasmimorpha longicaudata to host and host-habitat volatile cues. Entomol Exp Appl. 2012; 143(2):164–76.

38. Ovruski SM, Colin C, Soria A, Oroño LE, Schliserman P, Collin C. Introducción y producción en laboratorio de Diachasmimorpha tryoni y Diachasmimorpha longicaudata (Hymenoptera: Braconidae) para el control biológico de Ceratitis capitata (Diptera: Tephritidae) en la Argentina. Rev la Soc Entomológica Argentina. 2003; 62(3–4):49–59.

39. Viscarret MM, La Rossa R, Segura DF, Ovruski SM, Cladera JL. Evaluation of the parasitoid Diachasmimorpha longicaudata (Ashmead)(Hymenoptera: Braconidae) reared on a genetic sexing strain of Ceratitis capitata (Wied.)(Diptera: Tephritidae). Biol Control. 2006; 36(2):147–53.

40. Altschul SF, Gish W, Miller W, Myers EW, Lipman DJ. Basic local alignment search tool. J Mol Biol. 1990; 215(3):403–10. https://doi.org/10.1016/S0022-2836(05)80360-2 PMID: 2231712

41. Mannino MC, Rivarola M, Scannapieco AC, González S, Farber M, Cladera JL, et al. Transcriptome profiling of Diachasmimorpha longicaudata towards useful molecular tools for population management. BMC Genomics [Internet]. 2016; 17(1):793. Available from: https://doi.org/10.1186/s12864-016-2759-2 PMID: 27729028

42. Sievers F, Higgins DG. Clustal Omega, accurate alignment of very large numbers of sequences. In: Multiple sequence alignment methods. Springer; 2014. p. 105–16.

43. Hall TA. BioEdit: A User-Friendly Biological Sequence Alignment Editor and Analysis Program for Windows 95/98/NT. Nucleic Acids Symp. 1999;Series, 41:95–8.

44. Drummond AJ, Suchard MA, Xie D, Rambaut A. Bayesian phylogenetics with BEAUti and the BEAST 1.7. Mol Biol Evol. 2012; 29(8):1969–73. https://doi.org/10.1093/molbev/mss075 PMID: 22367748

45. Steel M, McKenzie A. Properties of phylogenetic trees generated by Yule-type speciation models. Math Biosci. 2001; 170(1):91–112. https://doi.org/10.1016/s0025-5564(00)00061-4 PMID: 11259805

46. Miller MA, Pfeiffer W, Schwartz T. Creating the CIPRES Science Gateway for inference of large phylogenetic trees. In: 2010 gateway computing environments workshop (GCE). Ieee; 2010. p. 1–8.

47. Pfaffl MW. Quantification strategies in real-time PCR. AZ Quant PCR. 2004; 1:89–113.

48. Xie F, Xiao P, Chen D, Xu L, Zhang B. miRDeepFinder: a miRNA analysis tool fordeep sequencing of plant small RNAs. Plant molecular biology 2012; 80 (1), 75–84.

49. Hellemans J, Mortier G, De Paepe A, Speleman F, Vandesompele J. qBase relative quantification framework and software for management and automated analysis of real-time quantitative PCR data. Genome Biol. 2007; 8(2):R19. https://doi.org/10.1186/gb-2007-8-2-r19 PMID: 17291332

50. Rieu I, Powers SJ. Real-time quantitative RT-PCR: design, calculations, and statistics. Plant Cell. 2009; 21(4):1031–3. https://doi.org/10.1105/tpc.109.066001 PMID: 19395682

51. Fire A, Xu S, Montgomery MK, Kostas SA, Driver SE, Mello CC. Potent and specific genetic interference by double-stranded RNA in Caenorhabditis elegans. Nature [Internet]. 1998; 391(6669):806–11. Available from: https://doi.org/10.1038/35888 PMID: 9486653

52. Wang S-N, Peng Y, Lu Z-Y, Dhiloo KH, Gu S-H, Li R-J, et al. Identification and expression analysis of putative chemosensory receptor genes in Microplitis mediator by antennal transcriptome screening. Int J Biol Sci. 2015; 11(7):737. https://doi.org/10.7150/ijbs.11786 PMID: 26078716

53. Zhou C-X, Min S-F, Yan-Long T, Wang M-Q. Analysis of antennal transcriptome and odorant binding protein expression profiles of the recently identified parasitoid wasp, Sclerodermus sp. Comp Biochem Physiol Part D Genomics Proteomics. 2015; 16:10–9. https://doi.org/10.1016/j.cbd.2015.06.003 PMID: 26164593

54. Ehrenberg S, Lewkowski O, Erler S. Dyeing but not dying: Colourful dyes as a non-lethal method of food labelling for in vitro-reared honey bee (Apis mellifera) larvae. J Insect Physiol. 2019; 113:1–8. https://doi.org/10.1016/j.jinsphys.2018.12.008 PMID: 30582906

55. Chen A, Zheng W, Zheng W, Zhang H. The effects of RNA interference targeting Bactrocera dorsalis ds-Bdrpl19 on the gene expression of rpl19 in non-target insects. Ecotoxicology. 2015; 24(3):595–603. https://doi.org/10.1007/s10646-014-1407-3 PMID: 25567188

56. Goelen T, Baets D, Kos M, Paulussen C, Lenaerts M, Rediers H, et al. Gustatory response and longevity in Aphidius parasitoids and their hyperparasitoid Dendrocerus aphidum. J Pest Sci (2004). 2018; 91 (1):351–60.

57. Li K-M, Ren L-Y, Zhang Y-J, Wu K-M, Guo Y-Y. Knockdown of Microplitis mediator odorant receptor involved in the sensitive detection of two chemicals. J Chem Ecol. 2012; 38(3):287–94. https://doi.org/10.1007/s10886-012-0085-y PMID: 22402893

58. Onchuru T. O., & Kaltenpoth M. (2019). Quantitative PCR primer design affects quantification of dsRNA-mediated gene knockdown. Ecology and Evolution, 9(14), 8187–8192. https://doi.org/10.1002/ece3.5387 PMID: 31380081

59. Montoya P, Liedo P, Benrey B, Barrera JF, Cancino J, Aluja M. Functional response and superparasitism by Diachasmimorpha longicaudata (Hymenoptera: Braconidae), a parasitoid of fruit flies (Diptera: Tephritidae). Ann Entomol Soc Am. 2000; 93(1):47–54.

60. Devescovi F. Estudios sobre el superparasitismo de larvas de la mosca del Mediterráneo Ceratitis capitata (Diptera: Tephritidae) por el parasitoide Diachasmimorpha longicaudata (Hymenoptera: Braconidae). Universidad de Buenos Aires. Facultad de Ciencias Exactas y Naturales; 2015.

61. Student. The probable error of a mean. Biometrika. 1908;1–25.

62. Mantel N. Evaluation of survival data and two new rank order statistics arising in its consideration. Cancer Chemother Rep. 1966; 50:163–70. PMID: 5910392

63. Forêt S, Maleszka R. Function and evolution of a gene family encoding odorant binding-like proteins in a social insect, the honey bee (Apis mellifera). Genome Res. 2006; 16(11):1404–13. https://doi.org/10.1101/gr.5075706 PMID: 17065610

64. Robertson HM, Gadau J, Wanner KW. The insect chemoreceptor superfamily of the parasitoid jewel wasp Nasonia vitripennis. Insect Mol Biol. 2010; 19:121–36. https://doi.org/10.1111/j.1365-2583.2009.00979.x PMID: 20167023

65. Peng Y, Wang S-N, Li K-M, Liu J-T, Zheng Y, Shan S, et al. Identification of odorant binding proteins and chemosensory proteins in Microplitis mediator as well as functional characterization of chemosensory protein 3. PLoS One. 2017; 12(7). https://doi.org/10.1371/journal.pone.0180775 PMID: 28732030

66. Lowe TM, Eddy SR. tRNAscan-SE: a program for improved detection of transfer RNA genes in genomic sequence. Nucleic Acids Res. 1997; 25(5):955–64. https://doi.org/10.1093/nar/25.5.955 PMID: 9023104

67. Tvedte ES, Walden KKO, McElroy KE, Werren JH, Forbes AA, Hood GR, et al. Genome of the Parasitoid Wasp Diachasma alloeum, an Emerging Model for Ecological Speciation and Transitions to Asexual Reproduction. Genome Biol Evol [Internet]. 2019; 11(10):2767–73. Available from: https://pubmed.ncbi.nlm.nih.gov/31553440 https://doi.org/10.1093/gbe/evz205 PMID: 31553440

68. Tang Liu, Yu Zhao, Lu. De Novo Transcriptome Identifies Olfactory Genes in Diachasmimorpha longicaudata (Ashmead). Genes (Basel). 2020; 11:144.

69. Zhou J-J, Huang W, Zhang G-A, Pickett JA, Field LM. "Plus-C" odorant-binding protein genes in two Drosophila species and the malaria mosquito Anopheles gambiae. Gene. 2004; 327(1):117–29. https://doi.org/10.1016/j.gene.2003.11.007 PMID: 14960367

70. Iovinella I, Dani FR, Niccolini A, Sagona S, Michelucci E, Gazzano A, et al. Differential expression of odorant-binding proteins in the mandibular glands of the honey bee according to caste and age. J Proteome Res. 2011; 10(8):3439–49. https://doi.org/10.1021/pr2000754 PMID: 21707107

71. Wang S-N, Shan S, Liu J-T, Li R-J, Lu Z-Y, Dhiloo KH, et al. Characterization of antennal chemosensilla and associated odorant binding as well as chemosensory proteins in the parasitoid wasp Microplitis mediator (Hymenoptera: Braconidae). Sci Rep. 2018; 8(1):1–11. https://doi.org/10.1038/s41598-017-17765-5 PMID: 29311619

72. Glatz R. Molecular Basis of Olfaction (Volume 130) (Progress in Molecular Biology and Translational Science (Volume 130)). 2015;1st Editio:144.

73. Zhao Y, Wang F, Zhang X, Zhang S, Guo S, Zhu G, et al. Transcriptome and expression patterns of chemosensory genes in antennae of the parasitoid wasp Chouioia cunea. PLoS One. 2016; 11(2). https://doi.org/10.1371/journal.pone.0148159 PMID: 26841106

74. Hausser J, Mayo A, Keren L et al. Central dogma rates and the trade-off between precision and economy in gene expression. Nat Commun. 2019; 10, 68. https://doi.org/10.1038/s41467-018-07391-8 PMID: 30622246

75. Wagner A. Energy Constraints on the Evolution of Gene Expression, Molec.Bio. and Evol. 2005; 22 (6): 1365–1374. https://doi.org/10.1093/molbev/msi126 PMID: 15758206

76. Oliveira DS, Brito NF, Franco TA, Moreira MF, Leal WS, Melo ACA. Functional Characterization of Odorant Binding Protein 27 (RproOBP27) From Rhodnius prolixus Antennae. Front Physiol [Internet]. 2018; 9(1175). Available from: https://www.frontiersin.org/article/10.3389/fphys.2018.01175 PMID: 30210359

77. Lapierre LR, Gelino S, Meléndez A, Hansen M. Autophagy and lipid metabolism coordinately modulate life span in germline-less C. elegans. Curr Biol. 2011; 21(18):1507–14. https://doi.org/10.1016/j.cub.2011.07.042 PMID: 21906946

78. Dall KB, Færgeman NJ. Metabolic regulation of lifespan from a C. elegans perspective. Genes Nutr. 2019; 14(1):1–12. https://doi.org/10.1186/s12263-019-0650-x PMID: 31428207

79. Schroeder EA, Brunet A. Lipid profiles and signals for long life. Trends Endocrinol Metab. 2015; 26(11):589–92. https://doi.org/10.1016/j.tem.2015.08.007 PMID: 26439976

80. Johnson AA, Stolzing A. The role of lipid metabolism in aging, lifespan regulation, and age-related disease. Aging Cell. 2019; 18(6):e13048. https://doi.org/10.1111/acel.13048 PMID: 31560163

81. Leal W. Deciphering the Rosetta Stone of Insect Chemical Communication. Am Entomol. 2014;60.

82. Swanson WJ, Vacquier VD. The rapid evolution of reproductive proteins. Nat Rev Genet. 2002; 3(2):137–44. https://doi.org/10.1038/nrg733 PMID: 11836507

83. Matsuo T. Rapid Evolution of Two Odorant-Binding Protein Genes, Obp57d and Obp57e, in the Drosophila melanogaster Species Group. Genetics [Internet]. 2008; 178(2):1061–72. https://doi.org/10.1534/genetics.107.079046 PMID: 18245367

84. Brand P, Ramírez SR, Leese F, Quezada-Euan JJG, Tollrian R, Eltz T. Rapid evolution of chemosensory receptor genes in a pair of sibling species of orchid bees (Apidae: Euglossini). BMC Evol Biol. 2015; 15(1):176.

85. Campanini EB, de Brito RA. Molecular evolution of Odorant-binding proteins gene family in two closely related Anastrepha fruit flies. BMC Evol Biol. 2016; 16(1):198. https://doi.org/10.1186/s12862-016-0775-0 PMID: 27716035

86. Shen J, Hu L, Dai J, Chen B, Zhong G, Zhou X. Mutations in pheromone-binding protein3 contribute to pheromone response variations in Plutella xylostella (L.) (Lepidoptera: Plutellidae). Pest Manag Sci. 2019;75. https://doi.org/10.1002/ps.5498 PMID: 31140683

87. Kowcun A, Honson N, Plettner E. Olfaction in the Gypsy Moth, Lymantria dispar Effect of pH, ionic strength, and reductants on pheromone transport by pheromone-binding proteins. J Biol Chem. 2001; 276(48):44770–6. https://doi.org/10.1074/jbc.M104688200 PMID: 11581252

88. Ishida Y, Leal WS. Cloning of putative odorant-degrading enzyme and integumental esterase cDNAs from the wild silkmoth, Antheraea polyphemus. Insect Biochem Mol Biol. 2002; 32(12):1775–80. https://doi.org/10.1016/s0965-1748(02)00136-4 PMID: 12429129

89. Laughlin JD, Ha TS, Jones DNM, Smith DP. Activation of pheromone-sensitive neurons is mediated by conformational activation of pheromone-binding protein. Cell. 2008; 133(7):1255–65. https://doi.org/10.1016/j.cell.2008.04.046 PMID: 18585358

90. Gong Y, Pace TCS, Castillo C, Bohne C, O'Neill MA, Plettner E. Ligand-interaction kinetics of the pheromone-binding protein from the gypsy moth, L. dispar: insights into the mechanism of binding and release. Chem Biol. 2009; 16(2):162–72. https://doi.org/10.1016/j.chembiol.2009.01.005 PMID: 19246007

91. Jeong YT, Shim J, Oh SR, Yoon HI, Kim CH, Moon SJ, et al. An odorant-binding protein required for suppression of sweet taste by bitter chemicals. Neuron. 2013; 79(4):725–37. https://doi.org/10.1016/j.neuron.2013.06.025 PMID: 23972598

92. Scheuermann EA, Smith DP. Odor-Specific Deactivation Defects in a Drosophila Odorant-Binding Protein Mutant. Genetics. 2019; 213(3):897–909. https://doi.org/10.1534/genetics.119.302629 PMID: 31492805

93. Xiao S, Sun JS, Carlson JR. Robust olfactory responses in the absence of odorant binding proteins. Elife. 2019; 8. https://doi.org/10.7554/eLife.51040 PMID: 31651397

94. Sun JS, Xiao S, Carlson JR. The diverse small proteins called odorant-binding proteins. R Soc Open Biol. 2018; 8(12):180208. https://doi.org/10.1098/rsob.180208 PMID: 30977439